TOWARDS COMBINED USE OF CHIRP SONAR AND PORTABLE PENETROMETER RESULTS AT THE POTOMAC RIVER

Reem Jaber, Department of Civil and Environmental Engineering, Virginia Tech, 200 Patton Hall, Blacksburg, VA, USA, (281-223-8074). e-mail: reemj@vt.edu
Dennis Kiptoo, Department of Civil and Environmental Engineering, Virginia Tech, 200 Patton Hall, Blacksburg, VA, USA, (540-449-6449). e-mail: dkiptoo@vt.edu
Nina Stark, Department of Civil and Environmental Engineering, Virginia Tech, 200 Patton Hall, Blacksburg, VA, USA, (540-922-3951). e-mail: ninas@vt.edu
Navid Jafari, Department of Civil and Environmental Engineering, Louisiana State University, 3212D Patrick F. Taylor Hall, Baton Rouge, LA, USA, (225-578-8475). e-mail: njafari@lsu.edu
Nadarajah Ravichandran, Department of Civil Engineering, Clemson University, 202 Lowry Hall, Clemson, SC, USA, (864-656-2818). e-mail: nravic@clemson.edu

Keywords: portable free fall penetrometer, chirp sonar, site characterization, sediment strength.

ABSTRACT

Acoustic methods are commonly used offshore to determine bathymetry and to classify seabed soil types. For example, chirp sonar represents a non-invasive technique to display and assess the stratigraphy of the upper tens of meters of the seabed. In the framework of seabed sediment investigations, acoustic methods are also often combined with sediment sampling, coring, and cone penetration testing. Portable free fall penetrometers (PFFPs) utilize accelerometers and sometimes a pore pressure sensor to estimate the effective sediment strength and pore pressure responses in the uppermost meter of the seabed, respectively. In this study, data from the Potomac River is presented utilizing the PFFP *BlueDrop* and a *SyQwest Stratabox HD* chirp sonar system for the geotechnical investigation of sediment bed properties in a riverine setting. Special attention was given to the uppermost subsurface properties (i.e., in the upper tens of centimeters) which are considered challenging for many seabed sampling methods. Initial results suggest that sediment strength of the PFFP and backscatter intensity of the chirp sonar are correlated.

INTRODUCTION

Acoustic methods are standard for seabed site investigations and have made significant contributions to the knowledge and understanding of the seabed for many years. This is based to a large extent on the ability of acoustics methods to image large areas of the seafloor in a cost-effective and efficient way (Jackson and Richardson 2007). Acoustics have been used to provide high-resolution bathymetry, seabed morphology, and some estimates into geological and geotechnical seabed properties (Brown et al. 2010). However, an increasing demand has emerged on acoustics to provide accurate mapping of the seafloor and to provide information about the seafloor composition and geotechnical soil classification at different sediment depths (Saleh and Rabah 2016). This is still challenged by the fact that acoustic results are highly sensitive to a number of soil and environmental parameters and seabed sediments can exhibit stratification with regards to geotechnical parameters in thickness on the order of centimeters (Osler et al. 2011; Stark et al. 2011). This explains why acoustic sonars are still often complemented by core samples and/or cone penetration tests (CPT) for geotechnical site characterization. Compared to the acoustic methods, the sampling and physical testing slow site investigation down significantly, and increases the costs (Goff et al. 2004; Saleh and Rabbah 2016). Furthermore, core samples and CPTs may be inefficient to obtain accurate seabed surface conditions due to sensors resolutions and sensitivity, particularly in the case of very soft or loose

sediments. Portable free fall penetrometers (PFFP) have emerged as an in-situ, rapid, and economical tool for seabed investigation of the uppermost seabed layers. Results from PFFP has been utilized in geotechnical site characterization and sediment mapping, in addition to identifying vertical subaqueous soil layering (Mulukutla et al. 2011; Albatal and Stark 2017; Albatal et al. 2019). PFFPs also proved to be effective under strong hydrodynamic conditions and in difficult access areas.

Many studies have been focused on integrating the capabilities of acoustics and geotechnical engineering towards more accurate modeling of sound propagation with seabed morphology, accurate scour depth measurements post storms, better soil characterization, and eventually, develop direct correlations between geotechnical properties and backscatter intensities (Houlsby and Rock 1998; Holland 2002; Osler et al. 2006; Harris et al. 2008; Osler et al. 2011). This study will investigate the combined use of PFFP and chirp sonar in assessing local geomorphodynamics in the Potomac River. Initial analysis of the PFFP and chirp sonar data are studied and compared as a step towards an integration of both methods in seabed classification.

REGIONAL CONTEXT

The Potomac River runs over 620 km from West Virginia into the Chesapeake Bay, Virginia, with a drainage area of 38,000 km^2 (ICPRB 2019). This makes it the fourth largest river at the U.S. Atlantic coast in terms of area and the second largest tributary to Chesapeake Bay. The river watershed includes parts of four states, West Virginia, Virginia, Maryland and Pennsylvania, as well as the District of Columbia. The river is fed by two springs, one located at Fairfax Stone in West Virginia for the North Branch, and the other in Highland County in Virginia (ICPRB, 2019).

The survey took place from August 5 - 8, 2019, in Charles County, MD (N 38°26’16.19“, W 77°15‘48.08“). PFFP and chirp sonar were deployed along nine transects (Fig. 1). Although there is no close discharge gage to reflect the hydrodynamic conditions at the survey location, the closest USGS gage 01658000 is located near Pomonkey, MD, which is 23 km upstream of the survey site. The average weekly discharge rate during the survey week was 0.028 m^3/s, while the median daily statistic shows an average of 0.025 m^3/s for that week of August (NWIS 2019). However, during the first half of July, discharge rates exceeded 110 m^3/s due to an extreme flooding event that started on July 8 and resulted in high water levels along the Atlantic coast (NWIS 2019). The soil in the proximity of survey site, also referred to as the “coastal plain” represents a dissected, hilly plane with layers of stratified, unconsolidated gravel, sand, and clay sediments distributed irregularly (Cummins et al. 2011).

METHODS

Acoustic methods including the previously mentioned chirp sonar, side scan sonar (SSS), and acoustic Doppler current profiler (ADCP) were used along the PFFP transects for data collection in this survey. However, this paper will focus only on the initial interpretation of the PFFP and the chirp sonar results.

Portable Free Fall Penetrometer (PFFP)

The PFFP *“Bluedrop”* is a relatively light weight instrument (~7.7 kg and 63.1 cm long) that can be deployed from a small vessel in an easy and fast manner. The PFFP uses five accelerometers of ± 2 *g*, ± 18 *g*, ± 50 *g*, ± 200 *g* and ± 250 *g* capacities (with *g* being the gravitational acceleration) to continuously measure acceleration/deceleration at a rate of 2 kHz as the *Bluedrop* penetrates

into the soil (Stark et al. 2014b) . The penetrometer is also equipped with a pressure sensor at the u_2 position (behind the tip) to measure pore pressures up to 2 MPa.

The PFFP free falls through the water column under its own weight and penetrates into riverbed, where the soil resistance starts acting against the probe until it reaches a final penetration depth. The accelerometers are measuring the deceleration of the PFFP as it advances into the soil, and the deceleration-time histories are then used to derive the impact velocity and the penetration depth of the penetrometer through first and second integration (Dayal and Allen 1973; Stoll and Akal 1999; Stark and Wever 2009). Using Newton's second law, the force decelerating the PFFP calculated from the deceleration profiles is assumed to reflect the soil resistance solely neglecting other forces, and is divided by the area subjected to the load to get the bearing capacity. To account for the high penetration rate of the penetrometer in comparison with the standard constant rate of the CPT of 2 cm/s, the dynamic bearing capacity is corrected by a strain rate factor to obtain the quasi-static bearing capacity (*qsbc*) (Dayal and Allen 1973; Stark et al. 2014a).

Chirp sonar

The *SyQwest Stratabox HD* chirp sonar is an acoustic instrument that provides images of seabed stratigraphy with a vertical resolution of up to 6 cm. It can survey to a water depth of 150 m and penetrates the seabed up to 40 m (Stratabox HD manual 2016). Sound waves, generated from the projector also known as transducer, are transmitted into the sea in all directions at a ping rate of up to 10 Hz and are then returned to the projector as sonar echoes. The strength of the return signal and the time it needs to travel back are then processed to depict the desired output in terms of distance from the source and backscatter intensity. Measurements in shallow water (<1.5 m) are limited by the blanking distance effect of 1 m due to transducer location.

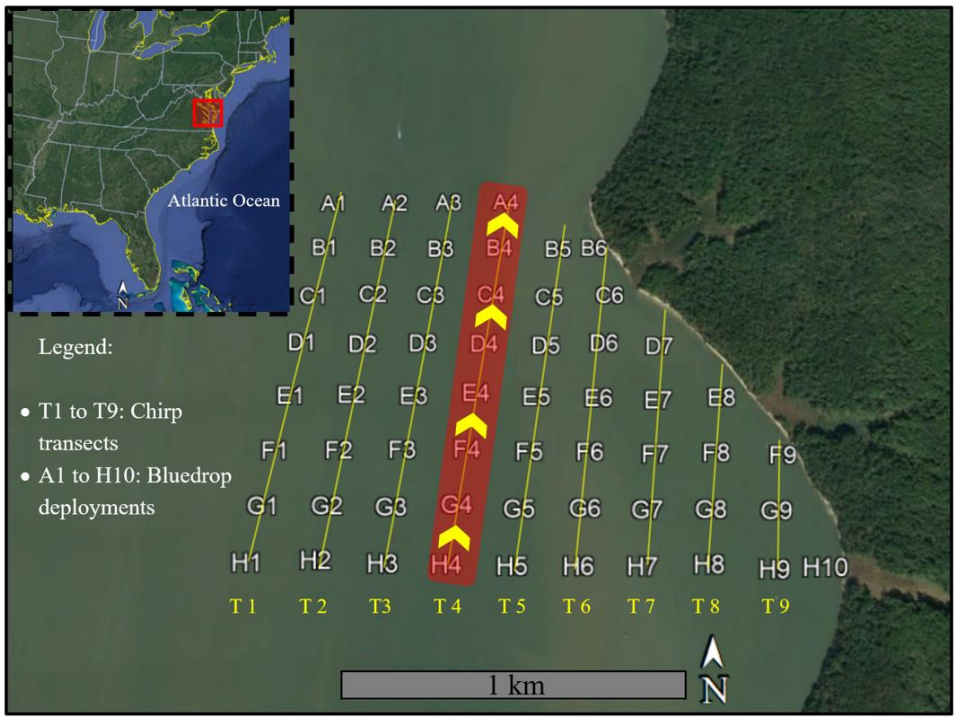

Fig. 1. Google earth image (2018) of the PFFP deployments and chirp sonar transects (38°26′16.19″N, 77°15′48.08″W). Transect T4 is focus of this study (Map data: Google, SIO, NOAA, U.S Navy, NGA, GEBCO, LDEO-Columbia, NSF, NOAA).

Sixty locations were surveyed along nine transects labeled from A to H (Fig. 1), with 2 drops per location and a total of 120 PFFP deployments. This paper will focus on comparing the PFFP and the chirp sonar data along transect T4 only (Fig. 1 red shaded). The chirp transect starts at H4 and ends at A4 (represented by yellow arrows), and the distance between each site is ~ 200 m.

Correlation between PFFP and Chirp data

Few studies have focused on a direct comparison between chirp sonar and PFFP data. However, several researchers have looked into correlations between acoustics signals and geotechnical soil properties. Osler (2002) correlated the first and second normal incidence of the acoustic signal return with a sediment classification technique based on the surface and volume scatter of the returned signal and their decay rate. Additionally, the chirp measurements have been empirically correlated with soil bulk properties such as the density, porosity, and shear strength using impedance, scattering models, and acoustic texture methods (Harris et al. 2008). Figure 2 provides a flow chart that summarizes the most used concepts in correlating between acoustic methods and geotechnical properties of the seabed based on Harris et al. (2008).

Return signals of the chirp sonar will vary in intensity as they reflect off different soil layers with different geotechnical properties. Higher backscatter intensity reflect minimal attenuation of the transmitted signal due to limited propagation in the soil layer. The limit of sound propagation is often correlated with the seabed soil type encountered at different depths. Therefore, higher backscatter intensities can represent harder objects and stiffer layers while lower backscatter intensities can represent softer objects and less stiff bottoms (Stratabox HD manual 2016).This study makes an initial attempt to correlate between the backscatter intensity of the chirp sonar and the *qsbc* values estimated by the PFFP.

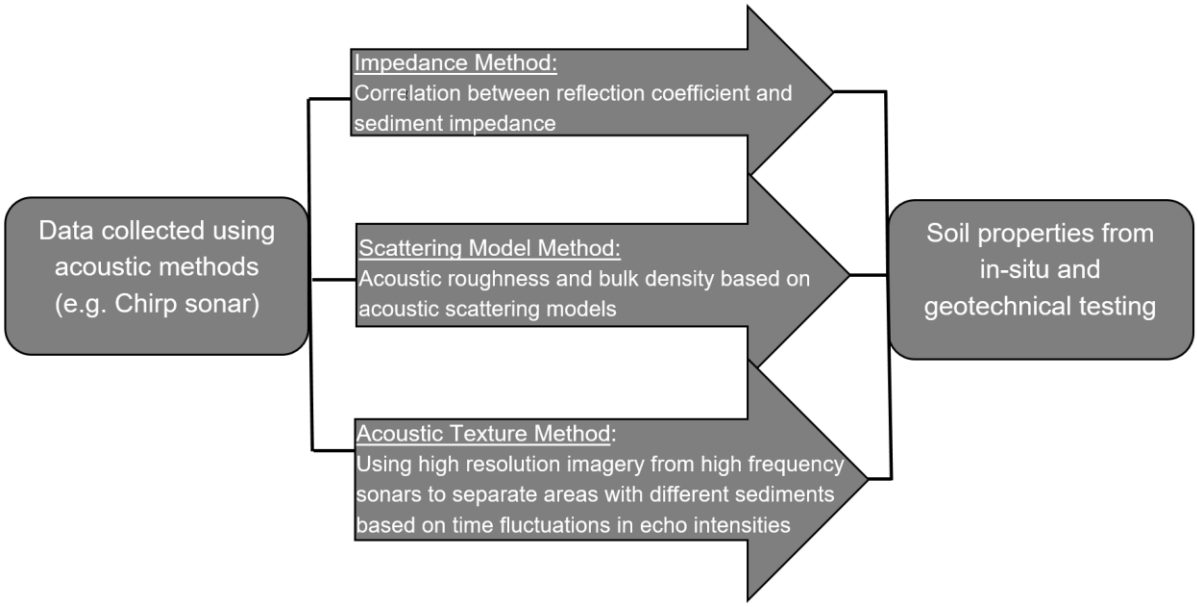

Fig. 2. Summary of methods developed to correlate between acoustics and soil properties after Harris et al (2008).

RESULTS AND DISCUSSION

Figure 3(a) displays an image of the PFFP instrument, and Fig. 3(b) shows an example of the PFFP output at site C4 including deceleration, impact velocity, and *qsbc* with the penetration

depth. At this location, the impact velocity as the penetrometer hits the riverbed is 5.13 m/s (at a penetration depth of 0 cm). The maximum deceleration and *qsbc* values are 2.7 *g* and 21.5 kPa, respectively, at a penetration depth of 66 cm.

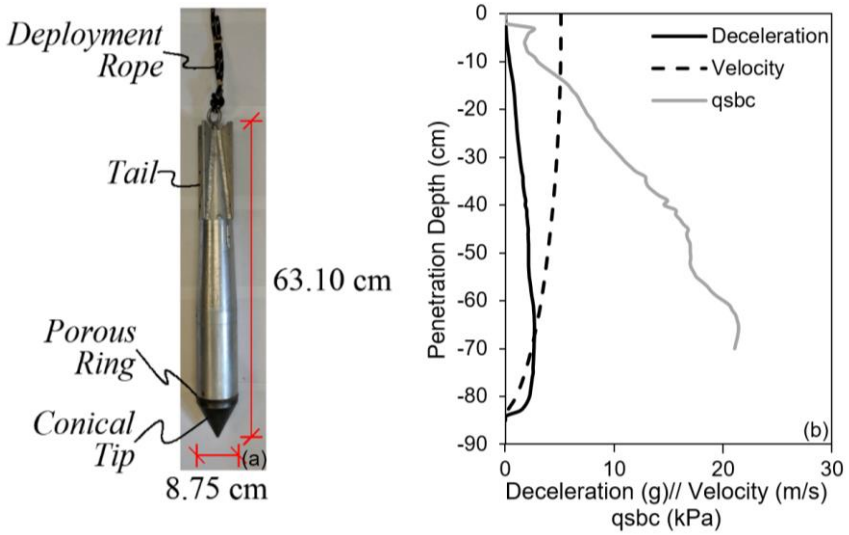

Fig. 3. (a) PFFP *BlueDrop* and (b) PFFP output deceleration, velocity and estimated *qsbc*-depth profiles at C4.

Figure 4(a) shows an example of the chirp sonar images along a short section of transect 4, starting from C4 upstream to A4. The *Bluedrop* deployments are shown in Fig. 4(b), with 2 drops per location. Visual observations during the survey and soil traces on the *Bluedrop* suggested the soil type at C4 to be different than the soil type at B4 and A4.

The water depth was estimated using the pressure recorded by the *Bluedrop* and the direct measurements of the chirp sonar. The water depth derivations from the PFFP were only corrected to account for Bernoulli's effect on the pressure with flow velocity. Also, the water depth displayed by the chirp was corrected to account for the chirp mounting technique on the side of the boat below the water level (~15 cm), and hence that same distance should be added to the water depth values. The corrected values measured by the chirp were 6.55 m, 4.55 m, and 4.75 m, respectively, while the PFFP analysis suggested 6.6 m, 4.4 m, and 4.8 m at C4, B4, and A4, respectively. This can be considered an excellent match considering that the Bernoulli correction is rather simplified regarding accounting for all fluid effects (e.g., Mumtaz et al. 2018). This suggests that the simplified Bernoulli correction provided more accurate results than reported in Stark and Ziotopoulou (2017), where the recorded pressure deviated from hydrostatic pressure by an additional calibration parameter *x* that had to be subtracted from the recorded pressure to reach matching results. This improvement could be related to environmental conditions or an improvement of pore pressure filter ring quality and saturation.

The *qsbc*-depth profiles of both deployments at each of the three locations are shown in Fig. 4. (b). The shape of the profiles, the penetration depth of the penetrometer, and the maximum *qsbc* reached are generally consistent between the two PFFP drops at each site, which provides confidence in the PFFP results and its ability to replicate results. Although this consistency was more evident at site C4, the deviation between the two drops at the other two sites is only observed at deeper layers and might be attributed to the spatial variation in soil properties due to the boat drift while dropping. At C4, the *qsbc* values increase steadily with penetration depth until a maximum of 21 kPa is reached at 66 cm below the riverbed. However, the *qsbc* of the soil at

sites B4 and A4 seem to increase less in the top subsurface layers (below 20 and 25 cm, respectively) followed by a rapid increase in the deeper layers until achieving a maximum. The maximum *qsbc* values at B4 and A4 were higher than C4 and were achieved at a shallower depth (27 cm and 47 cm) than at site C4, indicating a difference in sediment strength and possibly soil type. Furthermore, irregularities were displayed in the *qsbc*-depth profiles at B4 and A4 at penetration depths of 25 cm and 20 cm versus the smoother profile variations at C4. This may suggest the presence of shell hash. Overall, the soil at B4 and A4 appears stiffer than the soil at C4 in terms of slightly higher *qsbc* values and limited penetration of the PFFP. The soil types observed here agree with the expectations based on the visual observations and the irregular reported distribution of unconsolidated clay and sand at the "coastal plain" area.

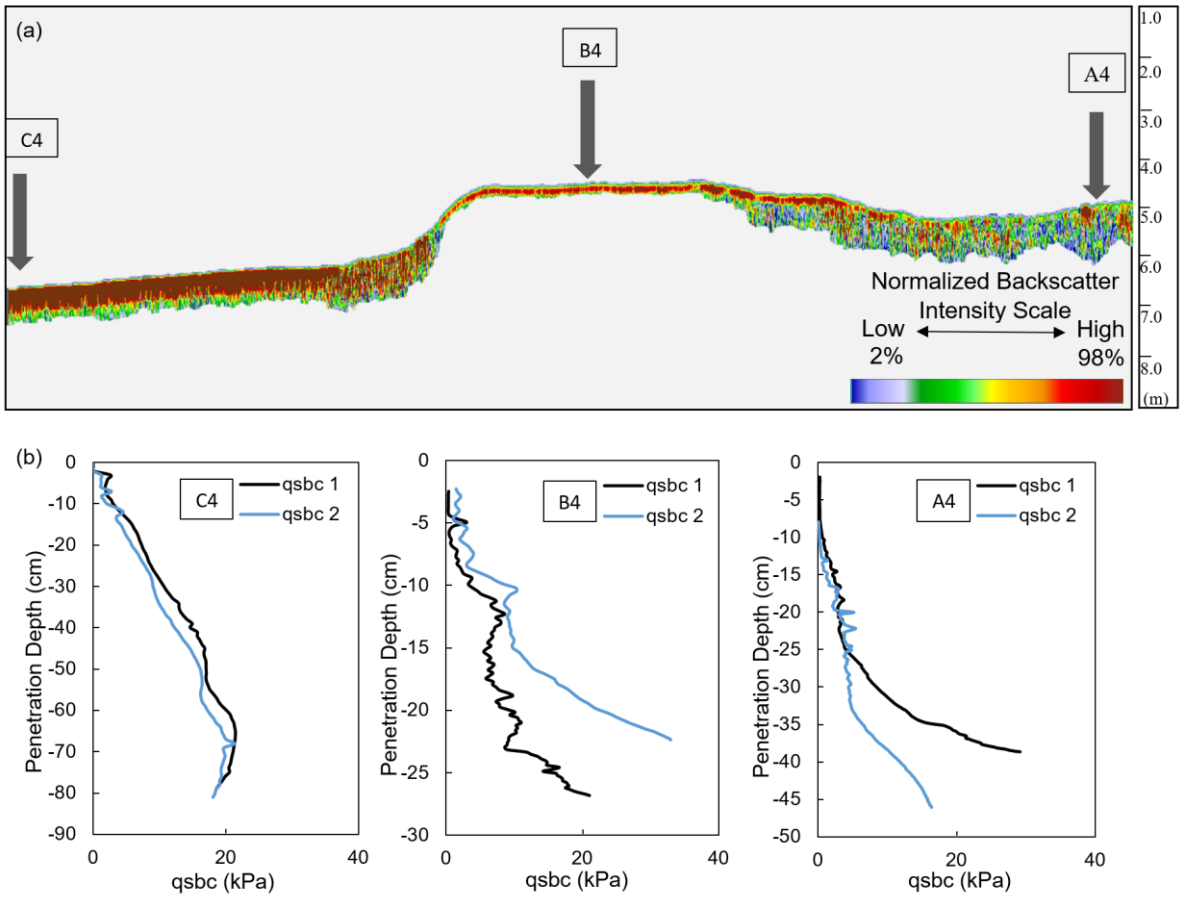

Fig. 4. (a) Chirp sonar image along transect T4 indicating locations of the three sites analyzed as shown by grey arrows. The color scale refers to different backscatter intensities ranging between blue and red color representing low and high backscatter intensities respectively. The grey color represents water column with depth values shown in the right side bar (y-axis). (b) PFFP deployment results at the three sites.

The output of the chirp results is represented in the form of normalized backscatter intensity (*NBI*), as a percentage of the maximum strength achieved by the return signal. As discussed earlier, higher backscatter intensities can generally indicate harder and stiffer soil layers. At C4, the first layer of the seabed is thin and displays a green color, indicating a low *NBI* value (between 20% and 50%) followed by a thicker layer ~ 40 cm showing high *NBI*, exceeding 75%. A deeper layer depicted at 7.2 m (~ 50 cm below riverbed) reflects *NBI* less than 50 %, with a transitional layer (yellow layer) in between with *NBI* ranging between 50% and 75%. The substratum at B4 was

detected at a water depth of 4.4 m showing an overall smaller portion of the riverbed strata ~ 40 cm. A similar top layer with low *NBI* was also observed at B4, followed by an increase in the backscatter intensity reflected by *NBI* values between 60 and 98% and a final layer with *NBI* less than 50%. Compared to site C4, most of the acoustic signal seem to be reflected early on at site B4, resulting in high NBI values at shallower depths. The rapid loss in the signal in the top soil layers (first 40 cm) may explain the change in the riverbed thickness displayed between the two sites at this low energy configuration of the sonar. Approaching A4 location, major changes in the backscatter intensity were observed. The layer of high *NBI* is discontinued here showing overall lower and less consistent *NBI*. Overall both the PFFP and the chirp sonar suggest variations in surficial soil conditions between the three sites.

For a better comparison between the PFFP and the chirp sonar, the *qsbc* and *NBI*-depth profiles are plotted on the same figure for the three sites, as presented in Fig. 5. These *NBI* values represent rather raw data. No further data reduction to account for noise and other impacts has been conducted yet. The high *NBI* values displayed by the chirp at C4 between 5 and 50 cm below the seabed does not seem to reflect the low *qsbc* values that did not exceed 20 kPa. This is possibly due to the constant gain used, which can be considered high in such weak soil type resulting in bottom reverberation effect, where the signal travels back and forth to the bottom several times and consequently fakes a stiff soil layering. This phenomenon is usually observed in shallow water depths due to minimal attenuation in the signal travelled. However, a weak soil layer as shown in the *qsbc*-depth profiles might also result in minimal losses in the reflected signal, producing the same effect as shallow water. At this point it is assumed that the high *NBI* layer is in fact a result from the sonar settings used. It will be explored if this can also be addressed through data processing techniques, but in future studies it is recommended to investigate different deployment configurations and settings. Nevertheless, it should be noted that this effect was most dominant in the softest and loosest clayey soils around location C4 and it appeared significantly less dominant at the more sandy location A4. It can also be seen that there are differences in the acoustic profiles for the different sites. However, a direct correlation between the *NBI* and the PFFP sediment resistance was not possible without further data processing and analysis procedures. Jaber et al. (2020*)* was able to obtain *NBI* and *qsbc* values at shallow sediment depths and compare them along a cross-river profile in the Brazos River, Texas. In that study, the authors found a favorable comparison in trend between the PFFP and the chirp. In this study, it appears that while differences in the chirp and the PFFP results agree on a change in river bed conditions, this direct comparison did not succeed over the sediment depth of the PFFP penetration due to the presence of the high *NBI* value layer in the raw data.

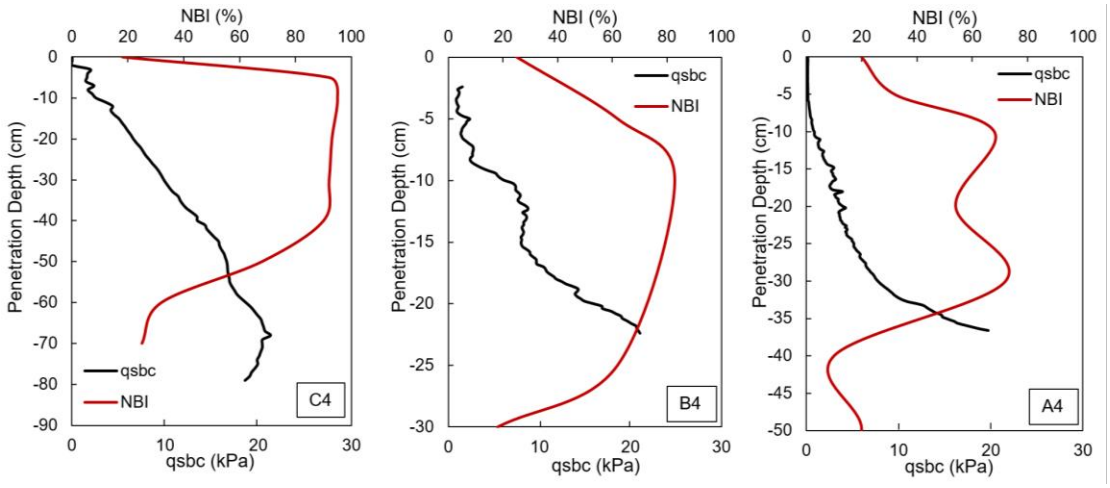

Fig. 5. Variations in the *qsbc* and the *NBI* values with penetration depth at the three sites.

CONCLUSION

This study presents a preliminary comparison between the deceleration, quasi-static bearing capacity profiles using portable free fall penetrometer and normalized backscatter intensity data using chirp sonar in the upper meter of the Potomac river bed during a survey in summer 2019. The investigated data set represents a small subset of the entire survey and the data reduction was limited, i.e., the compared data represent mostly direct measurement output data. The presented transect started towards the river center where sediments were clayey and transitioned towards sediments with higher sand content towards the shore. The PFFP results reflected clearly the differences in sediment type and associated river bed soil behavior in terms of differences in sediment strength and stratification. The normalized backscatter intensity also suggested differences in sediment conditions. Water depth estimated from both systems matched well. However, a direct match or correlation between the *qsbc* and the *NBI* could not been established here, due to the presence of a layer of high *NBI* values apparently masking results favorable for a direct comparison. It is assumed that this layer resulted from the deployment approach and configuration of the sonar system. Further steps will be taken regarding analyzing this data set and exploring pathways to address the issue of bias from the system configuration. Nevertheless, a relation between PFFP and the chirp sonar data, as theoretically expected, appears apparent, but more investigations are needed towards a direct correlation between the data products of the two systems. This is specifically motivated by the simplicity of the devices used during deployment being suitable for a wide range of vessels and environments.

ACKNOWLEDGMENTS

The authors would like to thank Strategic Environmental Research and Development Program (SERDP) for funding the field research presented here through grant MR-18-1233 and the National Science Foundation (NSF) for funding the data analysis through grant CMMI-1822307. The authors also like to acknowledge the efforts of Julie Paprocki, and the Coastal Hydrodynamics team at Virginia Institute of Marine Sciences for their data collection efforts in the field and particularly Grace Massey and Cristin Wright.

REFERENCES

Albatal, A., and Stark, N. 2017. Rapid sediment mapping and in situ geotechnical characterization in challenging aquatic areas. Limnology and Oceanography: Methods, 15(8), 690–705.

Albatal, A., Wadman, H., Stark, N., Bilici, C., & McNinch, J. 2019. Investigation of spatial and short-term temporal nearshore sandy sediment strength using a portable free fall penetrometer. Coastal Engineering, 143, 21-37.

Bilici, C., Stark, N., & Hajra, M. G. 2018. In situ geotechnical characteristics of surficial wetland waterway sediments. American Society of Civil Engineers, ASCE J. of Waterway, Port, Coastal, and Ocean Engineering, 144(6), 1-13.

Brown, C. J., Todd, B. J., Kostylev, V. E., & Pickrill, R. A. 2011. Image-based classification of multibeam sonar backscatter data for objective surficial sediment mapping of Georges Bank, Canada. Continental Shelf Research, 31(2), S110-S119.

Browne, T. M. 2010. Underwater acoustic imaging devices for portable scour monitoring. . Proceedings, 5th ICSE, San Francisco, November 7-10, 93.2 Overview of Underwater Imaging, 931-936.

Cummins, J., C. Buchanan, C. Haywood, H. Moltz, A. Griggs, C. Jones, R. Kraus, N. P. Hitt, and R. Bumgardner. 2011. Potomac Basin Large River Environmental Flow Needs. ICPRB Report 10-3. Interstate Commission on the Potomac River Basin. 7-8.

Dayal, U., & Allen, J. H. 1973. Instrumented impact cone penetrometer. Canadian Geotechnical Journal, 10(3), 397-409.

Gavin, K., and Prendergast J. L. 2018. Reliable performance indicators for bridge scour assessments. Proceedings of TU1406 Cost Action, Barcelona, September 27-28.

Goff, J. A., Kraft, B. J., Mayer, L. A., Schock, S. G., Sommerfield, C. K., Olson, H. C., Gulick, S. P. Nordfjord, S. 2004. Seabed characterization on the New Jersey middle and outer shelf: correlatability and spatial variability of seafloor sediment properties. Marine Geology, 209(1-4), 147–172.

Govindasamy, A. V., Briaud, J. L., Kim, D., Olivera, F., Gardoni, P., & Delphia, J. 2012. Observation method for estimating future scour depth at existing bridges. American Society of Civil Engineers, ASCE J. of Geotechnical and Geoenvironmental Engineering, 139(7), 1165-1175.

Harris, M. M., Avera, W. E., Abelev, A., Bentrem, F. W., & Bibee, L. D. 2008. Sensing shallow seafloor and sediment properties, recent history. Proceedings of Oceans 2008, Quebec City, September 15-18,1-11.

Interstate Commission on the Potomac River Basin. Potomac basin facts. https://www.potomacriver.org/potomac-basin-facts/. Accessed 19-10-26.

Jaber R., Stark N., Jafari N., Ravichandran, N. (2020). In-Situ Geotechnical Investigation of a Short Section of the Brazos River Post Hurricane Harvey Using a Portable Free Fall Penetrometer. Proceedings of Geocongress 2020, Minneapolis, February 25-28.

Mulukutla, G. K., Huff, L. C., Melton, J. S., Baldwin, K. C., McConnaughey, R. A., & Mayer, L. A. 2011. Erratum to: Sediment identification using free fall penetrometer acceleration-time histories. Marine Geophysical Research, 32(3), 413–413.

Mumtaz M.B, Stark N., Brizzolara S. 2018. Pore pressure measurements using a portable free fall penetrometer. Proceedings 4th International Symposium on CPT, June 21-22, Delft.

NWIS (National Water Information System) 2019. USGS current conditions for the nation-station 08114000. https://nwis.waterdata.usgs.gov/nwis/uv? Accessed 19-10-26.

Osler J.C., Hines P.C., Trevorrow M.V. 2002. Acoustic and *in-situ* techniques for measuring the spatial variability of seabed geoacoustic parameters in littoral environments. In: Pace N.G., Jensen F.B. (eds) Impact of Littoral Environmental Variability of Acoustic Predictions and Sonar Performance. Springer, Dordrecht, 81-89.

Prendergast, L.J. & Gavin, K., 2014. A review of bridge scour monitoring techniques. Journal of Rock Mechanics and Geotechnical Engineering, 6(2), 138-149.

Saleh, M., & Rabah, M. 2016. Seabed sub-bottom sediment classification using parametric sub-bottom profiler. NRIAG Journal of Astronomy and Geophysics, 5(1), 87–95.

Stark, N., and Wever, T.F. 2009. Unraveling subtle details of expendable bottom penetrometer (xbp) deceleration profiles. Geo-Marine Letters, 29(1), 39–45.

Stark, N., and Kopf, A. 2011. Detection and quantification of sediment remobilization processes using a dynamic penetrometer. Proceedings, MTS/IEEE KONA, Waikoloa, September 19-22, 1-9.

Stark N., Staelens P., Hay AE, Hatcher B., Kopf A. 2014a. Geotechnical investigation of coastal areas with difficult access using portable free-fall penetrometers. Proceedings 3rd International Symposium on CPT, Las Vegas, May 12-14.

Stark, N., Hay, A. E., & Trowse, G. 2014b. Cost-effective geotechnical and sedimentological early site assessment for ocean renewable energies. Proceedings 2014 Oceans-St. Johns, September 14-19, 1-8.

Stark, N., & Ziotopoulou, K. 2017. Undrained shear strength of offshore sediments from portable free fall penetrometers: theory, field observations and numerical simulations. Proceedings, 8th OSIG International Conference, London, September 12-14, Vol. 1, 391–399.

Stegmann, S., Villinger, H., and Kopf, A. 2006. Design of a modular, marine free-fall cone penetrometer. Sea Technology, (2), 27–33.

Stoll, R. D., and Akal, T. 1999. XBP - Tool for rapid assessment of seabed sediment properties. Sea Technology, 40(2), 47–51.

SyQwest 2016. StrataBox HD chirp operations and maintenance manual. https://www.syqwestinc.com/media/stratabox-3510/sboxmanual.pdf. Accessed 19-10-5.